

Modulation of carrier lifetime in MoS_2 monolayer by uniaxial strain

Hao Hong(洪浩), Yang Cheng(程阳), Chunchun Wu(吴春春), Chen Huang(黄琛), Can Liu(刘灿), Wentao Yu(于文韬), Xu Zhou(周旭), Chaojie Ma(马超杰), Jinhuan Wang(王金焕), Zhihong Zhang(张智宏), Yun Zhao(赵芸), Jie Xiong(熊杰), Kaihui Liu(刘开辉)

Citation: Chin. Phys. B . 2020, 29(7): 077201 . **doi:** 10.1088/1674-1056/ab99ba
Journal homepage: http://cpb.iphy.ac.cn; http://iopscience.iop.org/cpb

What follows is a list of articles you may be interested in

Effect of strain on exciton dynamics in monolayer WS_2

Lu Zhang(张璐), Da-Wei He(何大伟), Jia-Qi He(何家琪), Yang Fu(付洋), Yong-Sheng Wang(王永生)
Chin. Phys. B . 2019, 28(8): 087201 . **doi:** 10.1088/1674-1056/28/8/087201

How to characterize capacitance of organic optoelectronic devices accurately

Hao-Miao Yu(于浩淼), Yun He(何鋆)
Chin. Phys. B . 2018, 27(6): 067202 . **doi:** 10.1088/1674-1056/27/6/067202

Biaxial strain-induced enhancement in the thermoelectric performance of monolayer WSe_2

Wanhuizi Shen(沈婉慧子), Daifeng Zou(邹代峰), Guozheng Nie(聂国政), Ying Xu(许英)
Chin. Phys. B . 2017, 26(11): 117202 . **doi:** 10.1088/1674-1056/26/11/117202

Spin-valley Hall conductivity of doped ferromagnetic silicene under strain

Bahram Shirzadi, Mohsen Yarmohammadi
Chin. Phys. B . 2017, 26(1): 017203 . **doi:** 10.1088/1674-1056/26/1/017203

First-principles hybrid functional study of the electronic structure and charge carrier mobility in perovskite $CH_3NH_3SnI_3$

Li-Juan Wu(伍丽娟), Yu-Qing Zhao(赵宇清), Chang-Wen Chen(陈畅文), Ling-Zhi Wang(王琳芝), Biao Liu(刘标), Meng-Qiu Cai(蔡孟秋)
Chin. Phys. B . 2016, 25(10): 107202 . **doi:** 10.1088/1674-1056/25/10/107202

RAPID COMMUNICATION

Modulation of carrier lifetime in MoS_2 monolayer by uniaxial strain*

Hao Hong(洪浩)[1], Yang Cheng(程阳)[1], Chunchun Wu(吴春春)[1,2], Chen Huang(黄琛)[1], Can Liu(刘灿)[1], Wentao Yu(于文韬)[1], Xu Zhou(周旭)[1], Chaojie Ma(马超杰)[1], Jinhuan Wang(王金焕)[1,3], Zhihong Zhang(张智宏)[1], Yun Zhao(赵芸)[3], Jie Xiong(熊杰)[2], and Kaihui Liu(刘开辉)[1,†]

[1] *State Key Laboratory for Mesoscopic Physics and Frontiers Science Center for Nano-optoelectronics, Collaborative Innovation Center of Quantum Matter, School of Physics, Peking University, Beijing* 100871, *China*

[2] *State Key Laboratory of Electronic Thin Films and Integrated Devices, University of Electronic Science and Technology of China, Chengdu* 610054, *China*

[3] *School of Chemistry and Chemical Engineering, Beijing Institute of Technology, Beijing* 100081, *China*

(Received 18 May 2020; revised manuscript received 29 May 2020; accepted manuscript online 5 June 2020)

Carrier lifetime is one of the most fundamental physical parameters that characterizes the average time of carrier recombination in any material. The control of carrier lifetime is the key to optimizing the device function by tuning the electro–optical conversion quantum yield, carrier diffusion length, carrier collection process, *etc*. Till now, the prevailing modulation methods are mainly by defect engineering and temperature control, which have limitations in the modulation direction and amplitude of the carrier lifetime. Here, we report an effective modulation on the ultrafast dynamics of photoexcited carriers in two-dimensional (2D) MoS_2 monolayer by uniaxial tensile strain. The combination of optical ultrafast pump–probe technique and time-resolved photoluminescence (PL) spectroscopy reveals that the carrier dynamics through Auger scattering, carrier–phonon scattering, and radiative recombination keep immune to the strain. But strikingly, the uniaxial tensile strain weakens the trapping of photoexcited carriers by defects and therefore prolongs the corresponding carrier lifetime up to 440% per percent applied strain. Our results open a new avenue to enlarge the carrier lifetime of 2D MoS_2, which will facilitate its applications in high-efficient optoelectronic and photovoltaic devices.

Keywords: two-dimensional materials, carrier dynamics, strain, trap states

PACS: 72.20.Jv, 61.72.Hh **DOI:** 10.1088/1674-1056/ab99ba

1. Introduction

Reduced dimension brings two-dimensional (2D) transit ion metal dichalcogenides (TMDCs) many stimulating advantages, such as enhanced light–matter interaction,[1,2] unique physical properties,[3–7] and facile integration of hybrid structures.[8–10] With these features, TMDCs have led a revolutionary breakthrough in photodetectors,[11–13] optical modulators,[14] light-emitting diodes,[15,16] valleytronic devices,[17] *etc*. To realize and optimize those applications, understanding and engineering the photoexcited carrier dynamic processes are of paramount importance.[18–20] In TMDCs materials, the nonradiative rather than radiative relaxation pathways dominate the carrier dynamics.[21–23] Due to the large specific surface area and high density of defects, $\sim 43\%$ excitons will be trapped by surface defect states and only 2.8% excitons can exhibit radiative recombination.[24] This defect trapping process is ultrafast with time scale of a few picoseconds, which is comparable with the interlayer charge transfer ($\sim$ 1 ps)[25] and much faster than radiative recombination process (about hundreds of picoseconds).[23] Therefore, the defect trapping process rather than radiative recombination dominates the performances of TMDCs-based devices, such as charge collection efficiency, photoconductive gain, and response time. Many efforts have been devoted against the trap states. For example, the defect-mediated nonradiative recombination can be efficiently eliminated by decorating an organic superacid;[26] stacking graphene layer on TMDCs can selectively filter out the radiative recombination and enable pristine PL.[27] While it is still a challenge to directly prolong the lifetime of defect trapping process.

Benefiting from the high flexibility and toughness, strain has been regarded as a powerful route to effectively and continuously engineering the physical properties of TMDCs recently. The band structure,[28–32] phonon modes,[33,34] and the optical nonlinearity[35] can be significantly tuned. Under in-plane tensile strain, the strain-dependent carrier–phonon inter-

*Project supported by the Natural Science Foundation of Beijing, China (Grant No. JQ19004), the Excellent Talents Training Support Fund of Beijing, China (Grant No. 2017000026833ZK11), the National Natural Science Foundation of China (Grant Nos. 51991340 and 51991342), the National Key Research and Development Program of China (Grant Nos. 2016YFA0300903 and 2016YFA0300804), the Key Research and Development Program of Guangdong Province, China (Grant Nos. 2019B010931001, 2020B010189001, 2018B010109009, and 2018B030327001), the Science Fund from the Municipal Science & Technology Commission of Beijing, China (Grant No. Z191100007219005), the Graphene Innovation Program of Beijing, China (Grant No. Z181100004818003), the Fund from the Bureau of Industry and Information Technology of Shenzhen City, China (Graphene platform 201901161512), the Innovative and Entrepreneurial Research Team Program of Guangdong Province, China (Grant No. 2016ZT06D348), and the Fund from the Science, Technology, and Innovation Commission of Shenzhen Municipality, China (Grant No. KYTDPT20181011104202253).

†Corresponding author. E-mail: khliu@pku.edu.cn

© 2020 Chinese Physical Society and IOP Publishing Ltd

action in TMDCs has been fully studied and the corresponding nanosecond-scale lifetime is demonstrated to decrease slightly.[36,37] While a more comprehensive understanding of the modulation of carrier lifetime through the engineering of in-plane uniaxial strain is still lacking so far. Here, for the first time, we directly studied the modulation of the carrier dynamics in MoS_2 monolayer by uniaxial tensile strain. We found that the carrier dynamic process in MoS_2 has four channels (*i.e.*, Auger scattering, trap states scattering, carrier–phonon scattering, and radiative recombination process) with different time scales. Strain can significantly prolong the carrier lifetime associated with defect trapping by 440% per percent strain, while the other three carrier dynamic channels remain largely unchanged.

2. Method

MoS_2 monolayer samples were grown on 300-nm SiO_2/Si substrate by CVD method using MoO_3 and S powders as precursors. 10.0-mg MoO_3 powder was placed at the center of a tube furnace and 20-mg S powder at the upstream side 14 cm away from the MoO_3 powder. The CVD process was carried out in ultrahigh-purity Argon gas atmosphere under ambient pressure.

The CVD-synthesized MoS_2 monolayer was transferred onto flexible Acrylic substrate by the wet transfer method. PMMA (polymethyl methacrylate, 4%) in ethyl lactate solution was spin-coated onto MoS_2 and baked at 120 °C for 2 min. Then the sample was placed into KOH (1 M) aqueous solution at 80 °C for 5 min to lift off the PMMA/MoS_2 from the substrate. After thoroughly washing with deionized water for three times, the PMMA/MoS_2 film was transferred to the target acrylic substrate. At last, the PMMA/MoS_2/acrylic sample was dried naturally for several hours and baked at 80 °C for 10 min to enhance the interaction between MoS_2 and acrylic.

PL and Raman spectra were measured using self-built equipment with 532-nm CW laser. The integral time was set as 1 s for the PL measurements and 30 s for the Raman measurements with laser power of 1 mW.

We performed the pump–probe measurements with femtosecond pulses (∼ 100 fs, 80 MHz) generated by a Ti:sapphire oscillator (Spectra-Physics Mai Tai laser) and an optical parametric amplifier (OPO). In our pump–probe experiments, we pumped at 410 nm and probed at 670 nm. Those two pulses are separated in the time-domain by a controllable delay-time and focused onto the sample. After collection of the reflected pulses, 460-nm long-pass filter was used to filter out the pump pulse. The transient absorption signal, defined as $\Delta R/R = (R_{\text{with pump}} - R_{\text{without pump}})/R_{\text{without pump}}$, was recorded by a PMT and a lock-in amplifier with reflective geometry. The diameters of focused pump and probe pulse are ∼ 2 μm and ∼ 1 μm, respectively.

The time-resolved PL was excited by pulses from Ti:sapphire oscillator at 410 nm. We selected the PL signal of target wavelength by a 460-long-pass filter and a spectrometer (with resolution of ±2 nm) after photoexcitation and collection. Then, we acquired the time-resolved PL signal using single-photon APD (PicoQuant Company, TDA 200) combining with a TCSPC module (TimeHarp 260 PICO Single).

3. Result and discussion

In our experiments, uniaxial tensile strain was applied through bending the flexible acrylic substrate. The sample which is at the upper surface is stretched and the uniaxial tensile strain is applied by the friction force between the sample and substrate (Fig. 1(a)). Since acrylic has relatively large Young's modulus parameter and the interaction between acrylic and sample is large enough, the tensile strain can be efficiently transferred from substrate to the target sample. The strain amplitude can be simply estimated from the bending geometry of the acrylic by using the formula $\varepsilon = d/2r$, where d is the thickness of the acrylic and r is the curvature radius. Triangle-shaped MoS_2 flakes were grown by chemical vapor deposition methods on SiO_2/Si and then transferred on acrylic with the assistance of polymethyl methacrylate (PMMA) (Fig. 1(b)). Raman spectroscopy of MoS_2 flake shows two characteristic peaks around 400 cm^{-1}, which correspond to in-plane E^1_{2g} and out-of -plane A_{1g} phonon modes, respectively (Fig. 1(c)). The 18-cm^{-1} separation between these two peaks ($\omega_A - \omega_E$) indicates that our MoS_2 samples are monolayer in nature.[38]

The PL spectrum of MoS_2 monolayer features a prominent peak at ∼ 670 nm that corresponds to the A exciton radiative recombination at the K-valley in the Brillouin zone. Under imposition of tensile strain by bending the flexible acrylic substrate, the A exciton PL peak red shifts correspondingly (Fig. 1(d)). The shift slope is determined to be 16.9 nm/% strain and the relative change slope $(\lambda_\varepsilon - \lambda_0)/\lambda_0$ (where λ_ε and λ_0 stand for the PL peak wavelength with and without strain, respectively) is 0.023/% strain (Fig. 1(e)). Meanwhile, the PL spectrum also slightly broadens with strain. To quantify the broadening, we acquired the full width at half maximum (FWHM) of PL spectra and found that FWHM increases ∼ 1.3 nm/% strain.

To investigate the origin of PL broadening in MoS_2 under tensile stain, we applied time-resolved experiments to track the carrier dynamic processes in the following. The dynamics of photoexcited carriers in MoS_2 could be described by four processes as illustrated in Fig. 2(a): the first process with lifetime τ_1 of hundreds of femtoseconds is via Auger scattering; the second process with lifetime τ_2 of several picoseconds is attributed to the trapping by defect states; the third process is related with carrier-phonon scattering with lifetime τ_3 of tens

of picoseconds; and the last process is electron–hole radiative recombination with lifetime τ_4 of hundreds of picoseconds. In order to characterize the carrier lifetimes of these four processes with different time scales, we performed pump-probe measurements with high accuracy and time-resolved PL technique with large detection range. Figure 2(b) shows our experimental setup. One path of femtosecond pulses from Ti:sapphire oscillator at 820 nm was guided into an optical parametric oscillator (OPO) to generate wavelength-tunable probe laser, and another path with controlled time-delay was used as pump laser. The transient absorption signal of MoS_2 was recorded by photomultiplier (PMT) combining with a lock-in amplifier with reflective geometry, and the time-resolved PL signal was monitored by single-photon avalanche photodiode detector (APD) combining with time-correlated single photon counting (TCSPC) module.

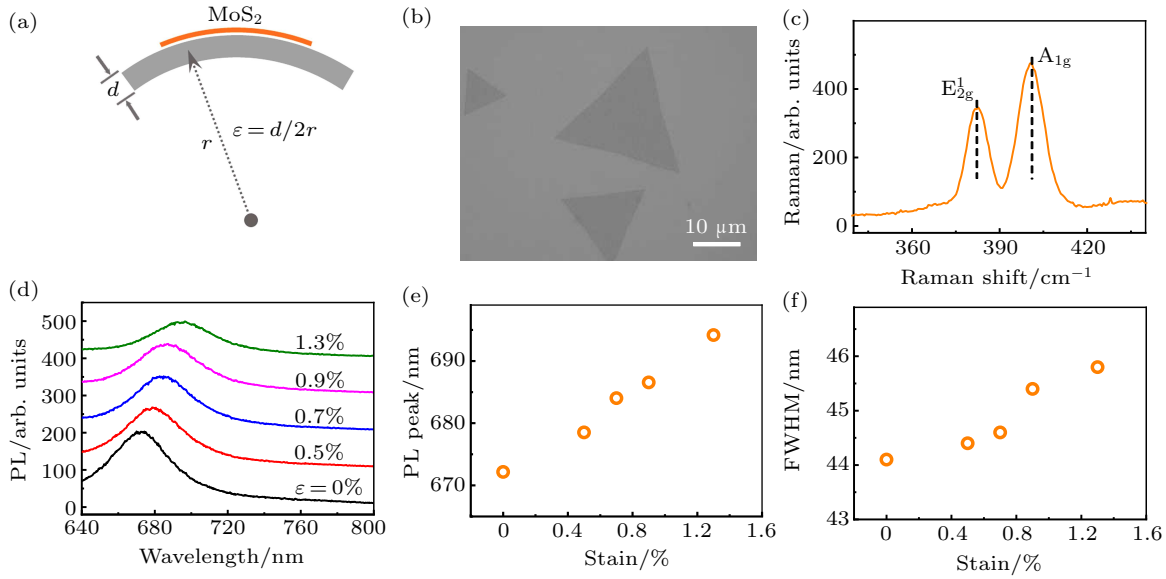


Fig. 1. PL and Raman spectra of MoS_2 monolayer under strain: (a) schematic illustration of strain apparatus, where the uniaxial tensile strain can be applied on MoS_2 by bending the flexible acrylic substrate. (b) Optical image of transferred MoS_2 monolayers on acrylic substrate. (c) Raman spectroscopy of monolayer MoS_2. The characteristic in-plane E^1_{2g} and out-of -plane A_{1g} phonon modes are labelled. (d) Strain-dependent PL spectra of monolayer MoS_2. (e) PL peak position under different strain amplitudes. The PL peak red shifts monotonically as the strain increases. (f) PL peak FWHM under different strain amplitudes. The imposition of tensile strain gently broadens the PL peak of MoS_2 monolayer.

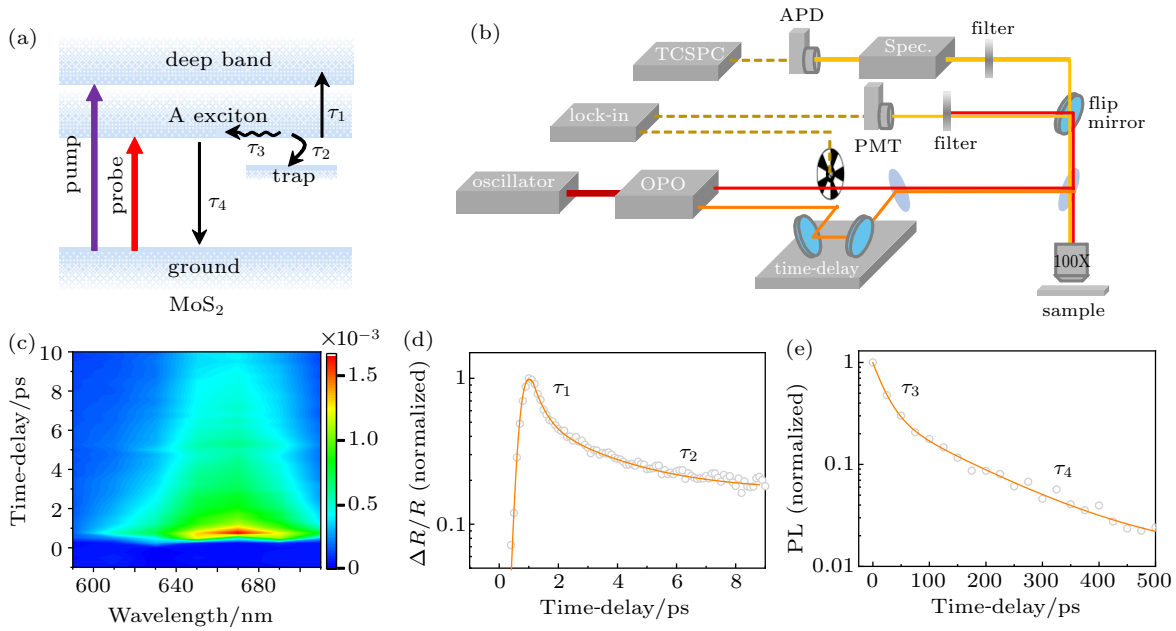


Fig. 2. Characterization of the carrier lifetime in MoS_2: (a) Illustration of four different channels for carrier recombination at the band edge of MoS_2 (*i.e.*, Auger scattering (τ_1), trap by defect states (τ_2), carrier–phonon scattering (τ_3), and electron–hole radiative recombination (τ_4)). (b) Schematics of the optical pump–probe and time-resolved PL setup. (c) The 2D plots of MoS_2 transient absorption at different probe wavelengths with pump wavelength of 410 nm. (d) Evolution of transient absorption signal with probe wavelength at 670 nm. The transient absorption signal undergoes biexponential decay with lifetimes of 0.38 ps and 2.3 ps, corresponding to lifetimes of Auger scattering and trapping by defect states respectively. (e) Time-resolved PL spectrum of MoS_2. The spectrum demonstrates the dynamic channels of carrier–phonon scattering and electron–hole radiative recombination, with lifetimes of 25 ps and 150 ps, respectively.

In the pump–probe experiment, we pumped MoS_2 by 410 nm pulse (width of $\sim$ 100 fs, fluence of 3 $\mu J/cm^2$) and probed the carrier population around the band gap with tunable wavelength of 590 nm–710 nm. The transient absorption signal of MoS_2 at different probe wavelengths and different pump–probe delay time is shown in the 2D mapping (Fig. 2(c)). Under horizontal cut of the 2D mapping, wavelength-dependent transient absorption presents a peak around 670 nm, which is consistent with the A exciton PL peak position shown in Fig. 1(d) (Fig. A1 in Appendix A). The vertical cut of the 2D mapping at 670 nm reveals the A exciton dynamics process (Fig. 2(d)). Transient absorption signal scales linearly with pump fluence, suggesting that nonlinear process such as exciton–exciton annihilation can be negligible under our experimental conditions (Fig. A2). From the logarithm plot of the transient absorption spectrum, we can observe that the A exciton dynamics performs two decay channels with two different slopes within the first 10 ps after photoexcitation. After fitting by Gaussian response function convoluted with a biexponential decay function, we can get the lifetime $\tau_1 = 0.38$ ps and $\tau_2 = 2.2$ ps. These two lifetimes are corresponding to the Auger scattering and defect trapping process, respectively.[24] For comparison, no obvious time-resolved signal could be observed for acrylic substrate (Fig. A3).

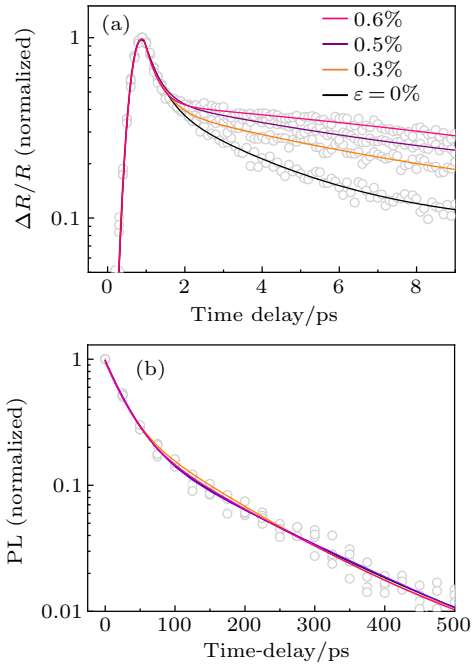


Fig. 3. Transient absorption and time-resolved PL spectra of MoS_2 monolayer under uniaxial tensile strain: (a) Strain-dependent transient absorption spectra of MoS_2 monolayer. Transient absorption spectra evolve significantly with strain. (b) Strain-dependent time-resolved PL spectra of MoS_2 monolayer. The time-resolved PL spectra remain largely unchanged under different strain amplitudes.

To obtain the slower carrier dynamic processes, we applied time-resolved PL and recorded the A exciton PL intensity under 410-nm pulse laser excitation. The A exciton PL dynamic process in the range of 0 ps–500 ps is shown in Fig. 2(e). Similarly, a biexponential decay trend can be observed and the lifetimes are fitted as $\tau_3 = 25$ ps and $\tau_4 = 150$ ps. These two lifetimes are determined as electron-phonon scattering and radiative recombination processes, respectively.[23]

After characterizing the carrier dynamic channels in MoS_2, we then investigated the modulation of carrier lifetimes by uniaxial strain. As the A exciton peak position varies with strain, the wavelength of probe pulse and the time-resolved PL were tuned correspondingly during strain to ensure that we were always detecting the A exciton dynamics. Strain-dependent transient absorption spectra are shown in Fig. 3(a). From the spectra, we can find the carrier dynamics evolve significantly with strain. While no significant change can be observed in the time-resolved PL spectra, which were recorded at the same time (Fig. 3(b)).

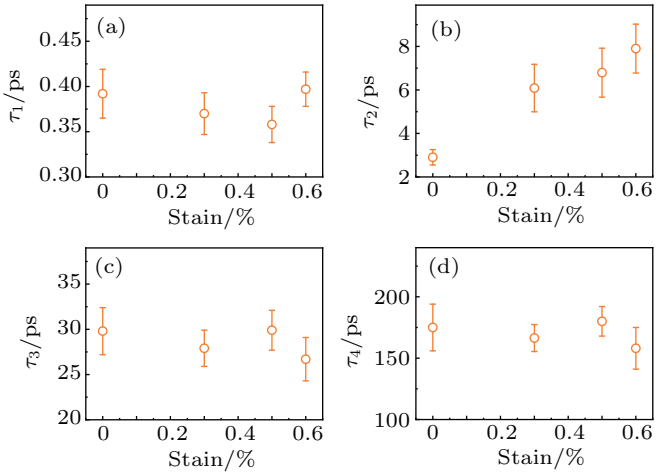


Fig. 4. Modulation of MoS_2 carrier lifetime by uniaxial tensile strain: (a)–(d) Evolution of Auger scattering lifetime τ_1 (a), defect trapping lifetime τ_2 (b), carrier–phonon scattering lifetime τ_3 (c), and electron–hole radiative recombination lifetime τ_4 (d) with strain in MoS_2 monolayer. The uniaxial tensile strain significantly prolongs defect trapping lifetime by 440% per percent applied strain, while hardly tunes the other three lifetimes. Error bars here describe standard errors of the fitting parameter.

To quantitatively analyze the strain engineering carrier dynamic processes, the measured transient absorption curves and time-resolved PL curves are fitted correspondingly. The strain-dependent fitting lifetimes are shown in Figs. 4(a)–4(d), from which we found quite different behaviors of lifetime variations: τ_2 significantly increases with strain, while the other three lifetimes remain largely unchanged within our resolution. For the defect trapping lifetime, the lifetime increases from $\sim$ 3 ps to $\sim$ 8 ps under 0.6% tensile strain, corresponding to 440% enhancement per percent strain. The relative change slope, defined as $\Delta\tau_\varepsilon/\tau_0 = (\tau_\varepsilon - \tau_0)/\tau_0$, is determined to be 2.8/% strain. Where τ_ε and τ_0 stand for the defect trapping lifetime with and without strain, respectively. Compared with the relative change of slope of the SHG intensity (-0.49/% strain),[35] PL (-0.025/% strain), and Raman (-0.012/% strain) peak positions,[28] this value is a few orders

higher, indicating that defect trapping process is much more sensitive with uniaxial tensile strain. While the Auger effect, electron–phonon coupling and radiative combination are independent of strain in MoS_2.

The rise of defect trapping lifetime is expected to enhance the PL intensity under strain. While from our experiment results, the PL intensity reduced slightly with strain increasing (Supplementary information in Fig. A4). That is because the tensile strain will lead a direct to indirect bandgap transition in MoS_2 at the same time.[28] Also, since only one of four lifetimes vary with strain, the radiative recombination with only proportion of 2.8% is hardly influenced. Even though, the prolongation of defect trapping process is very important for TMDCs-based devices. As the photoconductive gain is proportional to the defect trapping lifetime,[39] tensile strain will dramatically enhance the responsivity in a photoconductive detector. In a graphene/TMDCs/graphene heterostructure photodetector, where TMDCs serve as absorber and transfer the photoexcited carriers to graphene electrode, the charge transfer process with time scale of ~ 1 ps is comparable to the defect trapping process in TMDCs themselves, therefore significantly limiting the charge collection efficiency. With prolonging the defect trapping process to ~ 10 ps, the charge collection efficiency will be enhanced by a few times.

Currently we do not have a quantitative understanding on the strain-dependent defect trapping lifetime in MoS_2, and we believe more theoretical exploration on the strain modulation of carrier dynamics will be carried out and might provide more in-depth information in the near future. Strain-dependent lifetime under cryogenic temperature can be also very helpful, but it is quite technically challenging now and waiting for future investigations.

4. Conclusion

In conclusion, we have investigated the engineering of carrier lifetimes under uniaxial tensile strain in 2D MoS_2. We found that, in contrast to the carrier dynamics through Auger scattering, carrier–phonon scattering, and radiative recombination which are insensitive to applied strain, the defect trapping lifetime can be enlarged by 440% per percent strain. As the carrier dynamics processes are similar for different TMDCs, in-plane uniaxial strain is believed to be a universal approach for carrier lifetime engineering. Since the defect states dominate many physical processes in TMDCs, the prolongation of defect trapping lifetime can be very useful for optimizing the performances of TMDCs-based devices.

Appendix A: Supplementary information

Some experiment results and figures for better understanding the present article are given below.

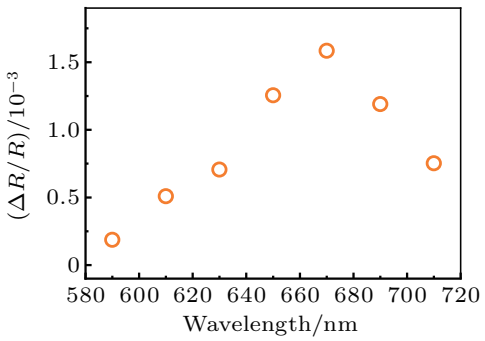


Fig. A1. Wavelength-dependent transient absorption signal of MoS_2 monolayer. From the horizontal cut of the 2D plot of MoS_2 transient absorption signal, we could find the wavelength-dependent transient absorption gives a peak around 670 nm, which is in accordance with A exciton PL peak position.

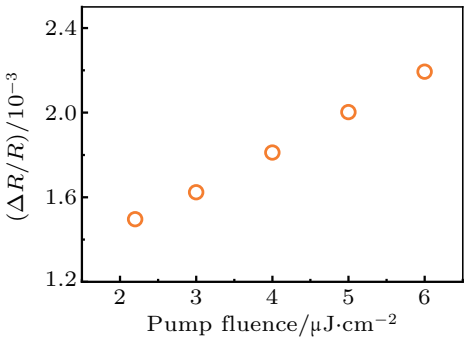


Fig. A2. Pump fluence-dependent transient absorption signal of MoS_2 monolayer. The transient absorption signal scales almost linearly with pump fluence, implying that only linear absorption is involved in this process, excluding the nonlinear effects such as exciton–exciton annihilation.

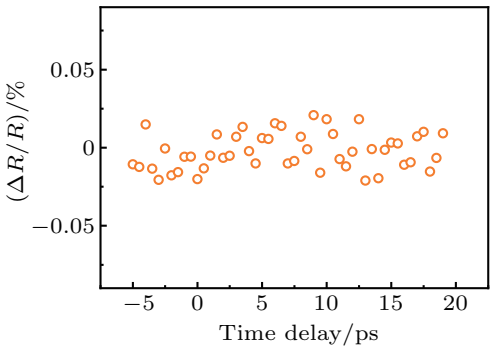


Fig. A3. Transient absorption signal of acrylic substrate. With the same pump–probe conditions as for MoS_2 monolayer in Fig. 2(d) in the text, no obvious time-resolved signal could be observed for acrylic substrate.

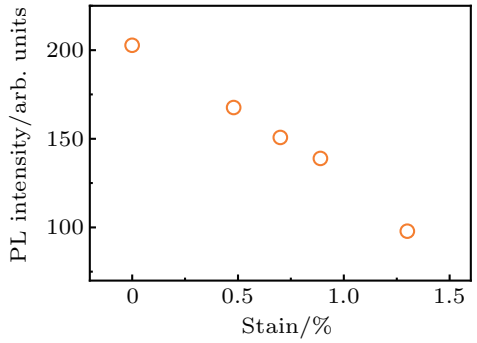


Fig. A4. Strain-dependent PL intensity of MoS_2 monolayer. The PL intensity reduces as the strain increases.

References

[1] Mak K F, Lee C, Hone J, Shan J and Heinz T F 2010 *Phys. Rev. Lett.* **105** 136805

[2] Splendiani A, Sun L, Zhang Y B, Li T S, Kim J, Chim C Y, Galli G and Wang F 2010 *Nano Lett.* **10** 1271

[3] Zeng H L, Dai J F, Yao W, Xiao D and Cui X D 2012 *Nat. Nanotechnol.* **7** 490

[4] Mak K F, He K L, Shan J and Heinz T F 2012 *Nat. Nanotechnol.* **7** 494

[5] Cao T, Wang G, Han W P, Ye H Q, Zhu C R, Shi J R, Niu Q, Tan P H, Wang E, Liu B L and Feng J 2012 *Nat. Commun.* **3** 887

[6] Ye Z, Cao T, O'brien K, Zhu H, Yin X, Wang Y, Louie S G and Zhang X 2014 *Nature* **513** 214

[7] Yang H, Kim S W, Chhowalla M and Lee Y H 2017 *Nat. Phys.* **13** 931

[8] Novoselov K S, Mishchenko A, Carvalho A and Castro Neto A H 2016 *Science* **353** aac9439

[9] Liu C, Hong H, Wang Q, Liu P, Zuo Y, Liang J, Cheng Y, Zhou X, Wang J and Zhao Y 2019 *Nanoscale* **11** 17195

[10] Cheng Y, Huang C, Hong H, Zhao Z and Liu K 2019 *Chin. Phys. B* **28** 107304

[11] Yu W J, Liu Y, Zhou H, Yin A, Li Z, Huang Y and Duan X 2013 *Nat. Nanotechnol.* **8** 952

[12] Britnell L, Ribeiro R, Eckmann A, Jalil R, Belle B, Mishchenko A, Kim Y J, Gorbachev R, Georgiou T and Morozov S 2013 *Science* **340** 1311

[13] Massicotte M, Schmidt P, Vialla F, Schädler K G, Reserbat-Plantey A, Watanabe K, Taniguchi T, Tielrooij K J and Koppens F H 2016 *Nat. Nanotechnol.* **11** 42

[14] Sun Z, Martinez A and Wang F 2016 *Nat. Photon.* **10** 227

[15] Ross J S, Klement P, Jones A M, Ghimire N J, Yan J, Mandrus D, Taniguchi T, Watanabe K, Kitamura K and Yao W 2014 *Nat. Nanotechnol.* **9** 268

[16] Pospischil A, Furchi M M and Mueller T 2014 *Nat. Nanotechnol.* **9** 257

[17] Schaibley J R, Yu H, Clark G, Rivera P, Ross J S, Seyler K L, Yao W and Xu X 2016 *Nat. Rev. Mater.* **1** 16055

[18] Mouri S, Miyauchi Y and Matsuda K 2013 *Nano Lett.* **13** 5944

[19] Zhang L, Chu W, Zheng Q, Benderskii A V, Prezhdo O V and Zhao J 2019 *J. Phys. Chem. Lett.* **10** 6151

[20] Sun Y, Meng Y, Dai R, Yang Y, Xu Y, Zhu S, Shi Y, Xiu F and Wang F 2019 *Opt. Lett.* **44** 4103

[21] Korn T, Heydrich S, Hirmer M, Schmutzler J and Schüller C 2011 *Appl. Phys. Lett.* **99** 102109

[22] Wang R, Ruzicka B A, Kumar N, Bellus M Z, Chiu H Y and Zhao H 2012 *Phys. Rev. B* **86** 045406

[23] Shi H Y, Yan R S, Bertolazzi S, Brivio J, Gao B, Kis A, Jena D, Xing H G and Huang L B 2013 *ACS Nano* **7** 1072

[24] Aleithan S H, Livshits M Y, Khadka S, Rack J J, Kordesch M E and Stinaff E 2016 *Phys. Rev. B* **94** 035445

[25] He J Q, Kumar N, Bellus M Z, Chiu H Y, He D W, Wang Y S and Zhao H 2014 *Nat. Commun.* **5** 5622

[26] Amani M, Lien D H, Kiriya D, Xiao J, Azcatl A, Noh J, Madhvapathy S R, Addou R, Santosh K and Dubey M 2015 *Science* **350** 1065

[27] Lorchat E, López L E P, Robert C, Lagarde D, Froehlicher G, Taniguchi T, Watanabe K, Marie X and Berciaud S 2020 *Nat. Nanotechnol.* **15** 283

[28] Conley H J, Wang B, Ziegler J I, Haglund Jr R F, Pantelides S T and Bolotin K I 2013 *Nano Lett.* **13** 3626

[29] He K, Poole C, Mak K F and Shan J 2013 *Nano Lett.* **13** 2931

[30] Desai S B, Seol G, Kang J S, Fang H, Battaglia C, Kapadia R, Ager J W, Guo J and Javey A 2014 *Nano Lett.* **14** 4592

[31] McCreary A, Ghosh R, Amani M, Wang J, Duerloo K A N, Sharma A, Jarvis K, Reed E J, Dongare A M and Banerjee S K 2016 *ACS Nano* **10** 3186

[32] Ji J, Zhang A, Xia T, Gao P, Jie Y, Zhang Q and Zhang Q 2016 *Chin. Phys. B* **25** 077802

[33] Doratotaj D, Simpson J R and Yan J A 2016 *Phys. Rev. B* **93** 075401

[34] Li T H, Zhou Z H, Guo J H and Hu F R 2016 *Chin. Phys. Lett.* **33** 046201

[35] Liang J, Zhang J, Li Z, Hong H, Wang J, Zhang Z, Zhou X, Qiao R, Xu J and Gao P 2017 *Nano Lett.* **17** 7539

[36] Niehues I, Schmidt R, Drüppel M, Marauhn P, Christiansen D, Selig M, Berghäuser G, Wigger D, Schneider R and Braasch L 2018 *Nano Lett.* **18** 1751

[37] Zhang L, He D, He J, Fu Y and Wang Y 2019 *Chin. Phys. B* **28** 087201

[38] Li H, Zhang Q, Yap C C R, Tay B K, Edwin T H T, Olivier A and Baillargeat D 2012 *Adv. Funct. Mater.* **22** 1385

[39] Yariv A 1997 *Optical electronics in modern communications*, 5th edn. (New York: Oxford University Press) p. 425